Radiation Measurements xxx (2013) 1–4

Contents lists available at SciVerse ScienceDirect

Radiation Measurements

journal homepage: www.elsevier.com/locate/radmeas

Cathodoluminescence of oxyfluoride glass-ceramics

U. Rogulis [a], E. Elsts [a,*], J. Jansons [a], A. Sarakovskis [a], G. Doke [a], A. Stunda [b], K. Smits [a]

[a] Institute of Solid State Physics, University of Latvia, 8 Kengaraga Street, 1063 Riga, Latvia
[b] Riga Biomaterials Innovation and Development Center, 3 Pulka Street, 1007 Riga, Latvia

HIGHLIGHTS

- ·We have studied Tb, Ce and Eu activated oxyfluoride glass-ceramics.
- Ce activated sample has the fastest cathodoluminescence decay times.
- X-ray excited luminescence shows, that Tb activated sample is the most intense.
- Intensity of Tb activated sample is 10 times smaller than intensity of CsI(Tl).

ARTICLE INFO

Article history:
Received 13 October 2012
Received in revised form
17 December 2012
Accepted 19 December 2012

Keywords:
Glass-ceramics
Cathodoluminescence
Decay times

ABSTRACT

Tb, Ce, Eu activated oxyfluoride glass-ceramics with the composition $SiO_2 \cdot Al_2O_3 \cdot Li_2O \cdot LaF_3$ have been studied by cathodoluminescence (CL). We compared CL intensities and decay times of the Tb, Ce, Eu activated glass-ceramic samples and observed that the Tb activated sample has the most intense luminescence, but the Ce activated sample has the shortest decay times. Induced optical absorption and thermostimulated luminescence have been observed after X-ray irradiation of samples.

1. Introduction

The advantages of glass-ceramics material over single crystal luminescent detectors and scintillators could be its low-cost and large-volume production possibilities. Nanocrystallites could be formed in oxyfluoride glass-ceramics if the proper thermal treatment procedures have been applied (Hu et al., 2005). The disadvantage of glass and glass-ceramic scintillators is their radiation damage limiting their application for precision calorimetry (Weber, 2002). It was shown in (Pan et al., 2008) that Tb activated glasses and glass-ceramics of composition $SiO_2 \cdot Al_2O_3 \cdot Li_2O \cdot LaF_3$ may have high scintillation efficiency; this efficiency is the highest for glass-ceramics; however, their decay times have not been reported.

Our recent cathodoluminescence (CL) studies of the spectra and decay times were done in the glass and glass-ceramics samples with the composition: $SiO_2 \cdot Al_2O_3 \cdot Na_2O \cdot LaF_3 \cdot NaF$, activated by terbium and ytterbium (Elsts et al., 2010). Cathodoluminescence spectra of the glasses and glass-ceramics show characteristic Tb^{3+} luminescence bands: 'blue' ($^5D_3 \rightarrow {}^7F_J$) and 'green' ($^5D_4 \rightarrow {}^7F_J$) groups. We observed 'blue' to 'green' group ratio changes, which could be explained by the cross-relaxation between Tb^{3+} ions.

In our previous work (Rogulis et al., 2012) we obtained characteristics of oxyfluoride samples $49SiO_2 \cdot 6Al_2O_3 \cdot 24Li_2O \cdot 20LaF_3$ activated with Tb, Ce, Eu by DTA (Differential thermal analyzer), CL (cathodoluminescence), XRD (X-ray diffraction), SEM (scanning electron microscope), EDS (energy dispersive X-ray spectroscopy) techniques. We found out that presence of crystalline phase enhances the CL of Tb activated samples significantly.

In this research we continued to study composition $48SiO_2 \cdot 6Al_2O_3 \cdot 24Li_2O \cdot 20LaF_3$ activated with terbium, cerium and europium. We summarized the results of all the cathodoluminescence decay times, compared the X-ray induced luminescence intensity with well known scintillator CsI (Tl). Formations of the radiation defects after X-ray irradiation have been observed by measuring induced optical absorption and thermo-stimulated luminescence.

2. Experimental

Samples were synthesized at the Institute of Solid State Physics from raw materials SiO_2, Al_2O_3, Li_2CO_3 and LaF_3 with the composition:

* Corresponding author. Tel.: +371 29977814; fax: +371. 67132778.
E-mail addresses: eelsts@cfi.lu.lv, eelsts@lu.lv (E. Elsts).

1350-4487/$ – see front matter © 2013 Elsevier Ltd. All rights reserved.
http://dx.doi.org/10.1016/j.radmeas.2012.12.020

$48SiO_2 \cdot 6Al_2O_3 \cdot 24Li_2O \cdot 20LaF_3 \cdot 2TbF_3$ (SALL:Tb),

$48SiO_2 \cdot 6Al_2O_3 \cdot 24Li_2O \cdot 20LaF_3 \cdot 2CeO_2$ (SALL:Ce),

$48SiO_2 \cdot 6Al_2O_3 \cdot 24Li_2O \cdot 20LaF_3 \cdot 2Eu_2O_3$ (SALL:Eu).

The powders of the components were mixed, and after that the mixture was heated at 800 °C for 1 h. Then the mixture was melted at 1400 °C for 1 h and liquid glass was cast. The temperatures for the following heat treatment were estimated from curves that have been taken with thermal analyzer DTG-60 (Rogulis et al., 2012). Samples have been heated at the temperature higher than DTA curve second crystallization temperature to obtain crystalline phase, that is, 750 °C for SALL:Tb, SALL:Ce and 800 °C for SALL:Eu. The Cathodoluminescence (CL) spectra and decay curves were measured and recorded by a ФЛУ-106 type photo-multiplier tube. Pulsed beam of 6 kV electrons was used for cathodoluminescence experiments. Phase composition of SALL ceramics has been investigated by the X-ray powder diffraction measured by X'Pert PRO diffractometer. After annealing at 750 °C for SALL:Tb, SALL:Ce and at 800 °C for SALL:Eu two types of crystalites have been observed: fluorides LaF_3 and silicates ($LiAlSiO_4$, $LiLaSiO_4$) – for experimental details see Rogulis et al. (2012). Thermally stimulated luminescence (TSL) measurements were carried out using X-ray irradiation (W anode, 30 kV, 10 mA) at liquid nitrogen temperature and heating the samples in the 85–600 K range. The X-ray excited luminescence spectra were recorded by Andor Shamrock B303-I spectrograph equipped with a CCD camera (Andor DU-401A-BV). The surfaces of all samples were equal size. Optical absorption spectra at room temperature have been measured using spectrophotometer Specord 210 - 2.

3. Results and discussion

We have measured cathodoluminescence spectra (Fig. 1) and decay times (Fig. 2) of SALL:Tb, SALL:Ce and SALL:Eu glass-ceramics samples. SALL:Tb CL spectrum (Fig. 1a) has luminescence bands at following wavelengths: 380 nm, 415 nm, 435 nm, 460 nm, 490 nm, 545 nm, 585 nm and 620 nm. Peaks at the spectrum of terbium activated samples correspond to energy level transitions $^5D_3 \rightarrow {}^7F_J$ ($J = 6, 5, 4, 3$) and energy level transitions $^5D_4 \rightarrow {}^7F_J$ ($J = 6, 5, 4, 3$) of the Tb^{3+}. SALL:Ce CL spectrum (Fig. 1b) has the most intense luminescence peak at 400 nm and additional peaks at 300 nm, 510 nm and 705 nm. Peak at 400 nm corresponds to energy transition $^2F_{5/2} \rightarrow {}^2F_{7/2}$ of the Ce^{3+}. SALL:Eu CL spectrum (Fig. 1c) has luminescence bands at following wavelengths: 577 nm, 589 nm, 613 nm, 651 nm and 702 nm that correspond to energy level transitions $^5D_0 \rightarrow {}^7F_J$ ($J = 0, 1, 2, 3, 4$) of the Eu^{3+}. No measurable CL of europium in the Eu^{2+} state has been observed at shorter wavelength region up to 400 nm (not shown).

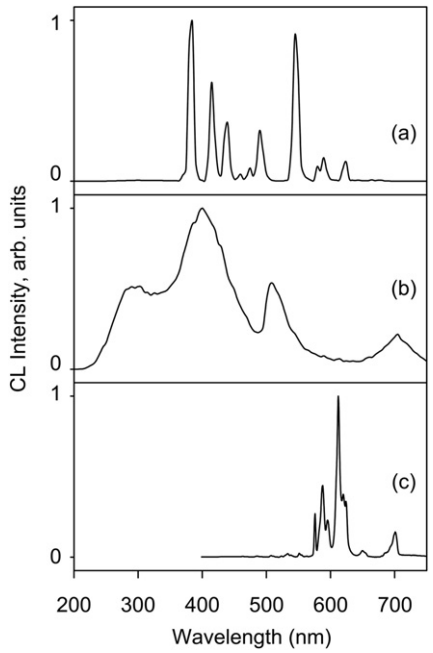

Fig. 1. CL spectra of SALL samples doped with Tb (a), Ce (b) and Eu (c).

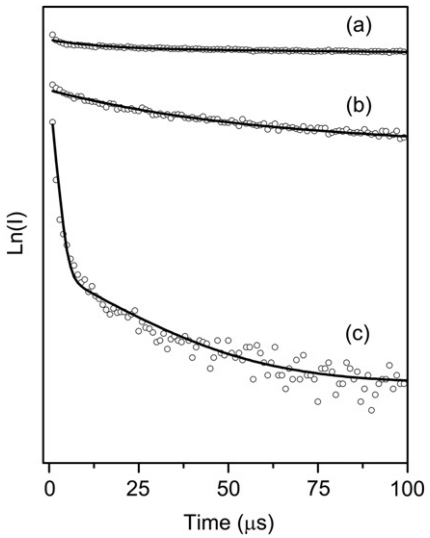

Fig. 2. CL decay curves of SALL:Tb (a) measured at 545 nm, SALL:Eu (b) measured at 613 nm and SALL:Ce (c) measured at 400 nm. Circles represent the experimental data and solid lines represent fitted curves.

CL decay curves (Fig. 2) can be sufficiently well approximated by two exponents – fast and slow:

$$f(t) = A_1 \exp(-t/\tau_1) + A_2 \exp(-t/\tau_2) + B, \quad (1)$$

A_i – the decay amplitude, B – constant, τ_i – decay time.

The decay times of the pairs of the exponents are listed in Table 1. For more convenient comparison of the exponential functions of different samples we have calculated the average exponents of each pair. For this purpose the following formula was used (from Tiseanu et al., 2009):

$$\langle \tau \rangle = \sum_{i=1}^{n} A_i \tau_i^2 / \sum_{i=1}^{n} A_i \tau_i. \quad (2)$$

We could not perform successful fitting of experimental decay time curves by the hyperbolic function or by only one exponent function.

Table 1
CL decay times of ceramic samples SALL:Tb, SALL:Ce, SALL:Eu measured at corresponding wavelengths. CL decay curves have been approximated by two components: fast τ_1 and slow τ_2. Average decay time τ_{av} is given as well.

Glass-ceramic samples	Wavelength (nm)	Average decay times (μs)		
		τ_1	τ_2	τ_{av}
SALL:Tb	545	290	2400	2360
SALL:Tb	385	3	840	6
SALL:Ce	400	0.3	4.0	1.7
SALL:Eu	613	25	200	170

Please cite this article in press as: Rogulis, U., et al., Cathodoluminescence of oxyfluoride glass-ceramics, Radiation Measurements (2013), http://dx.doi.org/10.1016/j.radmeas.2012.12.020

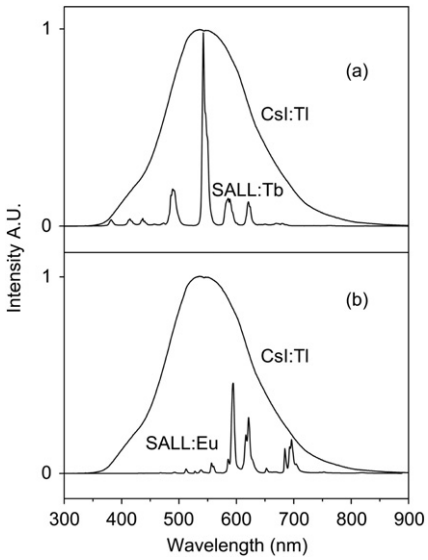

Fig. 3. The intensity of the X-ray induced luminescence of SALL:Tb sample part (a) and SALL:Eu sample part (b) compared to the well known scintillator CsI(Tl) sample of the same size.

In order to get explanation for the observed two different CL decay components we considered the following points. Charged particles and photons interacting with the lattice create electron–hole pairs, which afterward migrate to the luminescence centers. Crystals are more effective materials for transportation of electrons and holes (Pan et al., 2008; Nikl, 2006). Material point defects, flaws and surfaces can delay migration (Nikl, 2006), inhomogeneities also make decay times longer. Therefore, the slowest decay time component could be related to a retrapping of the electrons or holes by traps with different activation energies before they reach activator (Tb, Ce, Eu).

To get estimation about the order of magnitude of the scintillator efficiency of the investigated glass-ceramics, we have measured X-ray induced luminescence spectra of the SALL:Tb, SALL:Ce, SALL:Eu samples (Fig. 3), calculated the integrated area of the spectral curve and compared it with well-known scintillator CsI (Tl). CsI (Tl) has light yield (Light Yield): 60,000 photon/MeV and decay time ~1 μs (Tavernier et al., 2006). The most intense peak of the SALL:Tb sample is located at almost the same wavelength as the maxima of the luminescence CsI(Tl), but the integrated area of the spectral curve is about 11 times smaller. For the other glass-ceramics samples: the intensity at the peak of the SALL:Ce is 166 times lower than CsI (Tl) peak intensity, the intensity at the peak of the SALL:Eu is about half of the CsI (Tl) peak intensity, but the integrated area is 19 times smaller.

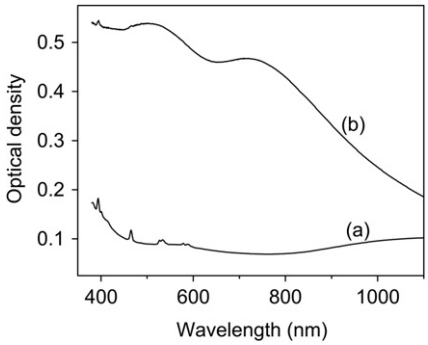

Fig. 4. Optical density of the SALL:Eu ceramic sample before irradiation (a) and after X-ray irradiation at RT (b).

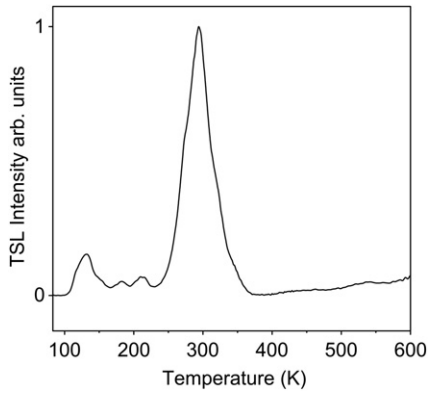

Fig. 5. Thermostimulated luminescence intensity of the ceramic sample after irradiation at 77 K, measured at 585 nm wavelength.

We observed that CL of investigated glass-ceramics slightly decreases with time. The reason for this process could be creation of radiation defects. Therefore, we have measured the optical density spectra of SALL:Eu sample (Fig. 4). We observed that after the X-ray irradiation for 1 h optical density rises to about 0.5 at 388–580 nm; induced absorption shows two broad defect absorption bands, which may affect the luminescence intensity of investigated glass-ceramics.

The creation of the defect trap centers in SALL:Eu is also confirmed by the X-ray induced thermostimulated luminescence measurements (Fig. 5), we observed that the most intense signal appears at room temperature (300 K) with the lowest measured peak at 133 K. The nature of defect trap centers observed by the optical absorption and TSL needs further investigations. For the scintillator applications, the induced absorption needs to be reduced.

4. Conclusions

We compared CL spectra and decay times of SALL:Tb, SALL:Ce, SALL:Eu ceramic samples. Decay times of studied samples could be well approximated by two exponential functions. SALL:Ce sample has the fastest decay times, but CL as well as the X-ray induced luminescence spectrum of the SALL:Tb sample is the most intense. Results of optical absorption and TSL show formation of the radiation defects after X-ray irradiation in the sample. The integral X-ray excited luminescence of the Tb activated glass-ceramics is about an order of magnitude less than that of the well-known scintillator crystal CsI(Tl).

Acknowledgments

Authors are grateful to Dr. L. Triklere for optical absorption measurements. This research is supported by the Latvian State Program for development of novel multifunctional materials.

References

Elsts, E., Rogulis, U., Jansons, J., Sarakovskis, A., 2010. Cathodoluminescence of terbium and ytterbium activated oxyfluoride glasses and glass ceramics. Latvian J. Phys. Tech. Sci. 5, 48–54.

Hu, Z.J., Wang, Y.S., Bao, F., Luo, W.Q., 2005. Crystallization behavior and microstructure investigations on LaF_3 containing oxyfluoride glass ceramics. J. Non-Crystalline Solids 351, 722–728.

Nikl, M., 2006. Scintillation detectors for X-rays. Meas. Sci. Technol. 17, 37–54.

Pan, Z., James, K., Cui, Y., Burger, A., Cherepy, N., Payne, S.A., Mu, R., Morgan, S.H., 2008. Terbium-activated lithium-lanthanum-aluminosilicate oxyfluoride

scintillating glass and glass-ceramic. Nucl. Instrum. Methods Phys. Res. A. 594, 215–219.
Rogulis, U., Elsts, E., Jansons, J., Sarakovskis, A., Doke, G., Stunda, A., Kundzins, K., 2012. Rare earth activated oxyfluoride glasses and glass-ceramics for scintillation applications. IEEE Trans. Nucl. Sci. 59. http://dx.doi.org/10.1109/TNS.2012.2212724
Tavernier, S., Gektin, A., Grinyov, B., Moses, W.W., 2006. Ion Detectors for Medical Applications. Springer, p. 332, Tavernier et al.
Tiseanu, C., Lórenz-Fonfría, V., Gessner, A., Kumke, M., Gagea, B., 2009. Comparative luminescence study of terbium-exchange dzeolites silylated with alkoxysilanes. J. Mater. Sci. Mater. Electron. 20, 312–316.
Weber, J., 2002. Inorganic scintillators: today and tomorrow. J. Lumin. 100, 35–45.

Please cite this article in press as: Rogulis, U., et al., Cathodoluminescence of oxyfluoride glass-ceramics, Radiation Measurements (2013), http://dx.doi.org/10.1016/j.radmeas.2012.12.020